NASA TECHNICAL TRANSLATION NASA TT F-16,082

METHODS OF NONSTATIONARY MEASUREMENT IN TURBINES

R. Larguier and A. de Sievers

Translation of "Méthodes de mesures instationnaires dans les turbomachines," Association Aéronautique et Astronautique de France,"Colloque d'Aérodynamique Appliquée, 10th, Université de Lille 1, Lille, France, Nov 7-9, 1973, 23 pp.

NATIONAL AERONAUTICS AND SPACE ADMINISTRATION
WASHINGTON, D.C. 20546 DECEMBER 1974

STANDARD TITLE PAGE

1. Report No. NASA TT F-16,082	2. Government Accession No.	3. Recipient's Catalog No.
4. Title and Subtitle METHODS OF NONSTATIONARY MEASUREMENT IN TURBINES		5. Report Date December 1974 6. Performing Organization Code
7. Author(s) R. Larguier and A. de Sievers, ONERA [Office National d'Etudes et de Recherches Aerospatiales]		8. Performing Organization Report No. 10. Work Unit No.
9. Performing Organization Name and Address Leo Kanner Associates, P.O. Box 5187 Redwood City, California 94063		11. Contract or Grant No. NASw-2481 13. Type of Report and Period Covered Translation
12. Sponsoring Agency Name and Address NATIONAL AERONAUTICS AND SPACE ADMINISTRATION, WASHINGTON, D.C. 20645		14. Sponsoring Agency Code

15. Supplementary Notes

Translation of "Méthodes de mesures instationnaires dans les turbomachines," Association Aéronautique et Astronautique de France, Colloque d'Aérodynamique Appliquée, 10th, Université de Lille 1, Lille, France, Nov. 7-9, 1973, 23 pp., (A74-25315)

16. Abstract The flow within an aircraft turbine contains numerous random and periodic-disturbances which can lead to performance losses, produce structural vibrations and generation noise. The present work describes techniques used by ONERA to measure transient parameters in subsonic and supersonic flows through aircraft turbines. Measurements of wall pressure distributions on rotor blades and in the inlet chamber upstream from the rotor are described along with hot-wire and pressure probe measurements of wake patterns.

17. Key Words (Selected by Author(s))	18. Distribution Statement
	Unclassified - Unlimited

19. Security Classif. (of this report)	20. Security Classif. (of this page)	21. No. of Pages	22. Price
Unclassified	Unclassified	31	

NASA-HQ

METHODS OF NONSTATIONARY MEASUREMENT IN TURBINES

R. Larguier and A. De Sievers*

1. Introduction

/2**

The flow within an aircraft turbine contains numerous random and periodic disturbances which can lead to performance losses, produce structural vibrations and generate noise. An analysis of these disturbances must therefore be included in any in-depth study of these machines.

Research by ONERA over the last few years has been directed toward the development of methods of nonstationary measurement applicable to aeronautic turbines. The main problems to be overcome arose from the high speed of the rotor blades, the small size of these blades, and safety restrictions.

Tests were performed from the subsonic to the supersonic range.

Following the directives of Chief Engineer P. Carrière, tests were begun on subsonic flows, the less problematic of the two types, using a model of an axial-flow compressor, operating on freon, built by the Energy Research Division of ONERA in Palaiseau. Freon was used in order to obtain supersonic flow at lower speeds than in air.

Some of the methods developed with these installations have already been put into service with the experimental aeronautic compressors used by SNECMA [Société Nationale d'Etudes et

---

*ONERA [Office National d'Etudes et de Recherches Aérospatiales; National Aerospace Study and Research Administration], Châtillon-sous-Bagneux, Hauts-de-Seine, France.

**Numbers in the margin indicate pagination in the foreign text.

de Constructions de Moteurs d'Avions; National Association of Aircraft Engine Research and Design]. The purpose of this discussion is to describe some of these methods and to give some of the results obtained. Some of these will be compared with the theoretical results.

These tests have been funded by the Research and Test /3
MethodsAAdministration of the Ministerial Armaments Delegation, under a general agreement with ONERA for the study of turbines.

The authors would like to thank IRME for allowing them to present this report.

2. Notation

p pressure

p_o upstream infinite pressure

q_o upstream infinite kinetic pressure in movable reference

p_q impact pressure

Δp nonstationary component of pressure

Δp_2 nonstationary component of impact pressure within axis reference considered (abs.: absolute reference; rel.: relative reference)

q kinetic pressure in the axis reference considered

$K_p z = (p_o - p)/q_o$: pressure coefficient

M Mach number

V speed within fixed reference

$\overline{V}$ average speed within fixed reference

$\Delta V = V - \overline{V}$

W speed within movable reference

$\overline{W}$ average speed within movable reference

$\Delta W = W - \overline{W}$

α speed orientation with fixed axes in relation to the meridian plane of the point (> 0 in the direction of rotation of the rotor)

$\bar{\alpha}$ average orientation of speed with fixed axes

$\Delta\alpha = \alpha - \bar{\alpha}$

β speed orientation with movable axes in relation to the meridian plane of the point (> 0 in the opposite direction from the direction of rotationoof the rotor)

$\bar{\beta}$ average speed orientation with movable axes

$\Delta\beta = \beta - \bar{\beta}$

d distance of a point from the testing plane located immediately downstream from the rotor

χ abscissa of the point of a profile measured over the length of a normalized chord BA-BF

l length of the normalized chord BA-BF /4

X,Y coordinates of points of profile in the systemsoffaxes OXY;

OY OY tangent to the profile set at 40% and normal to the axis of the rotor blade wheel

OX parallel to the axis of the rotor and passing through the point of tangency of OY with the profile

L chord of the profile in the system of axes OXY

Θ orientation of nonstationary probe in the calibration wind tunnel in relation to the direction of flow

Θ_1 orientation of nonstationary probe in the turbine, with an arbitrary point of origin

T elementary period (time interval between passage of two successive blades in front of the probe)

t time

t_o initial time corresponding to triggering of measurement device

Δt_o phase lead of measurements by cylindrical probe in comparison to hot-wire probe measurements

r local radius

R radius of outer fairing

ω angular velocity

N number of rotations per minute

U response of hot-wire anemometric probe

$\overline{U}$ average response of hot-wire anemometer

$\Delta U = U - \overline{U}$

$\sqrt{\overline{\Delta U^2}}/\overline{U}$: turbulence ratio

f(t) periodic component of signal to be analyzed

Q(t) random component of signal to be analyzed

3. Measurements in the Subsonic Range

3.1. Test Installation

The device [1] shown schematically in Fig. 1a is in the form of a small Eiffel wind tunnel 500 mm in diameter upstream from the rotor. The latter is driven by a 30-kW variable-speed electric motor. The air flow can be adjusted by "vanning" by means of a movable bellmouth downstream from the nozzle. The assembly is placed in a site divided into two compartments by a movable partition designed to prevent recycling of air (Fig. 1b). Air is aspirated to the outside through a dedusting filter for the purpose of obtaining favorable conditions for quantitative anemometric measurements by means of hot-wire microprobes.

The air is then sent to the upstream compartment /5 through a wide corridor with a soundproof lining. After passing through the nozzle, the air is discharged to the outside through a corridor similar to the entry corridor. The nozzle, which is broken up into fixed components, allows the device wide use flexibility.

In addition, the design of the throat, which is equipped with a deep honeycomb filter, and the careful design of the fairings have made it possible to obtain flows with excellent aerodynamic characteristics.

The speed distribution in the annular space upstream from the rotor blade wheel is quite uniform (Fig. 2). The characteristics of the turbulence measured upstream from the fairing of the hub are given in Fig. 3. These measurements were performed without the tranquilizing grating which can be added to the honeycomb filter of the throat.

3.2. Stationary Measurements of Pressure Distribution on Rotor Blades

These measurements were performed on a 20-blade conically generated rotor defined by the Energy Research Devision of ONERA [2] in such a way that the annular grid of rotor blades is characterized by a constant setting, camber and relative pitch from the blade roots to their tips (setting 40°, camber 32.5° and relative pitch 0.89). The marginal play provided between the rotor and the outer fairing is 0.5 mm.

Two diametrically opposed blades are equipped with pressure inlets along seven cross sections, each defined by the imaginary line of intersection of the blade and a circular cylinder coaxial with the rotor. These inlets are arranged along each cross section at homothetic abscissas, that is, along the same generatrices. The inlets with the same relative abscissas in the seven cross sections are connected by common pipes. Pressure measurements along a cross section are performed by first closing off the pressure inlets in the other cross sections by means of thin adhesive film. The pressure pipes exit within the axis of the blade root, pass through the rotor shaft and are connected to a pneumatic distributor affixed to the end of the shaft (Fig. 4). This distributor, designed and built by ONERA [3], is equipped with remote control allowing it to switch over each of the channels in turn to a pipe ending in a completely air-tight rotating joint, whose fixed part, supported by the bearing

of the machine, is connected to a differential manometric detector. All of these units are completely integrated into the fixed fairing upstream from the hub.

Figure 5 shows a few results of measurements involving three cross sections: r/R = 0.708, 0.834 and 0.918.

The measurements have been corrected for centrifugal effect.

To compensate for the lack of pressure inlets on the trailing edges of the blades, the pressure diagrams have been normalized by the value of the static pressure derived from radial measurements immediately downstream from the rotor. In addition it should be pointed out that the load torque derived from pressure integration is in satisfactory agreement with the motor torque.

The pressure distributions derived from the measurements are compared with those obtained by a two-dimensional computation on the basis of an ideal fluid [4].

The general configuration of the pressure distributions is appreciably the same; close to the periphery the computed values of K_p are higher than the measured values. The difference decreases and even tends to become inverted as one approaches the hub. Nevertheless the three-dimensional nature of the flow is quite apparent upon examination of the isobar curves represented on the developed surface of the blade (Fig. 6). Since the angle of attack of the blade and the relative speed increase from the hub to the periphery, as a result there is a corresponding increase in the load distribution along the span which is plainly shown by the isobar distribution. /6

The wall flow and especially the nature of the development of the boundary layer along the blade are closely related to potential flow. In addition, visualization of the transition on the outer skin by the sublimating coating method (Fig. 20) shows that the relative depth of the transition varies along the span (approximately 67% close to the hub and 51% close to the periphery).

3.3. Analysis of Rotor Wake Patterns

3.3.1. Measurement by Means of Hot-Wire Probes

The use of a crossed-wire probe was rejected due to practical considerations, and a method making use of an ordinary single-wire probe was used instead. This method required two successive measurements at a single point, the first directly furnishing the modulus of the local speed and the second its direction.

The modulus of the speed is determined by means of a probe whose wire is in a radial position (Fig. 7, Position A). To measure the orientation one need only follow up the preceding measurement with a single measurement by a probe whose wire is normal to the local radius (Fig. 7, Position B).

Preliminary wind-tunnel calibration of a probe whose pole is normal to the wind, using different orientations of the pole around its axis (Fig. 8), shows that the ratio of the response U to the flow speed V is solely a function of the angle of orientation θ.

Measurements of the speed and the angle as a function of time were performed in the same mode and were normalized by a rotor position reference (photoelectric cell detector).

These measurements were recorded, first, in analog form by photographing the screen of an oscilloscope equipped with a Polaroid camera, and second, in numeric form by means of a "numerical mean finder" [5].

This device, which is a sample recorder, restores the periodic component f(t) of the signal being analyzed by eliminating the random component Q(t).

The device is triggered by an electrical pulse delivered by the cell detecting the rotor position, and the signal is then examined by sampling. One hundred regularly spaced successive sample values are transmitted to 100 stores. Each time the device is triggered, the values of the 100 samples of the signal are accumulated in the corresponding stores with the previously stored values. Thus at the end of n passes the periodic component will be represented by n times the value f(t), while the random component, equal to the quadratic mean of n successive recordings, will have increased only in proportion to $\sqrt{n}$, with the result that the ratio f(t)/Q(t) will have improved in proportion to $\sqrt{n}$. The number of passes n is predetermined ($n_{max} = 999$). At the end of the recording process the stores are scrutinized in turn and the corresponding numerical values are transferred to perforated tape for subsequent processing by computer.

The oscillogram in Fig. 9, given as an example, shows, /7 on the one hand, the response of the hot wire during the elementary period T (step between two blades), and on the other, a visualization of the mean value of the same signal furnished by the mean finder. This mean represents 900 passes over a single blade.

Figure 10 shows the results of measurements at 3000 rpm, obtained with three different positions along a single radius located 10 mm downstream from the marginal profiles of the blades.

These are given in a system of fixed axes and in a system of movable axes linked to the rotor and are based on passage of a single channel in front of the probe.

The abscissa scale is graduated in relative values, t/T of the elementary period T, equal to one ms. The angles of the speed vector α and β are defined in Fig. 10a. It should be noted that with fixed axes, a decrease in relative speed in the wake is manifested both by a strong variation in the angle of deviation of the flow and by a variation in the speed modulus.

The deviation effect will obviously disappear in the unseparated zones after transposition to movable axes. An appreciable variation in the angle β persists, primarily close to the hub, where the presence of fluctuating airstream separations may in addition be detected by direct observation of the trace of the signal generated by the hot-wire probe on the oscilloscope screen.

Similar measurements were performed at various distances downstream from the rotor in order to determine the path and diffusion of the wake. Figures 11a, 11b and 11c showsthe results of measurements taken at different relative radii. Each of these figures shows the speedswwithin the wake for a single blade in movable axes at four different distances from the rotor. The abscissa scale represents the curvilinear distance, along an arc of a circle with the radius involved,

from the intial position of the probe (as recording is begun) and its position at the end of time t. In order to evaluate the twist of the wake, a second scale whose unit is the elementary period T (graduation t/T) has been superimposed over the axes of the abscissas.

The path of the wake in movable axes is appreciably helicoidal for each radius (rectilinear trace on the expanded graphs given in Figs. 11a, 11b and 11c).

However, the plash of the wake, which is virtually radial upon emission (trailing edge of blade), twists as it moves downstream. In addition, the thickness of the wake close to the hub is greater than it is toward the outer fairing and its diffusion is more marked.

3.3.2. Pressure Probe Measurements

The probe (Fig. 12) consisted of a cylindrical rod introduced radially into the turbine. A piezoelectric pickup (3) [6 and 7] placed in the body of the probe is connected to a pressure inlet opening (1) machined normal to the side wall. The dead space (2) between the pressure inlet and the pickup is very small, an arrangement which provides the device with a high passband.

Calibration of the probe with the impact tube yields its sensitivity coefficient and its transfer function.

Moreover, wind-tunnel calibration of a cylindrical probe of identical shape equipped with a stationary pressure detector yields the pressure distribution around the probe within the range of speeds occurring in the turbine.

From this one may derive a system of curves: /8

$$\frac{p}{p_2} = f(\theta, M) \qquad (S)$$

of the ratio between the pressure p/p_2 as a function of the relative orientation θ of the pressure inlet in relation to the axis of the flow and the Mach number of the flow M.

The probe is used in the turbine to record the response of the pickup as a function of time and the angle of orientation of the probe θ_1 in relation to an arbitrarily selected orientation.

Measurement of $p(t,\theta_1)$ is performed for several discrete values of θ_1 on either side of the mean direction of flow.

Time t is the time required to travel to the point of origin from a precisely defined point on the rotor.

A computer program automatically collects the experimental values $p(\theta_1)$ obtained for a single constant value of t. The program then uses the method of least squares to adjust these values on a curve p/p_2 of area (S).

This operation yields the fixed axes of the impact pressure p_2, the orientation of the speed and the Mach number of the flow at the instant t under consideration. It is repeated for 100 equidistant values of t over an elementary period T, the period of time between the passage of two successive blades.

The results obtained in this way in axes referred to the probe are additionally transferred to a system of axes referred to the rotor.

On an initial approximation, the tabulation procedure described above involves the assumption that the field of the flow around the probe at a given time matches that which would be observed with a uniform permanent flow of the same speed and orientation. Comparison of these results with the results obtained with the hot-wire probe will indicate the validity of this approximation.

As an example, Fig. 13 shows an oscillogram representing, first, the response of the probe during two elementary periods, and second, a visualization of the mean periodic value of a single signal summed 900 times by the mean finder, the probe being positioned downstream from the rotor wheel in the same location as the hot-wire probe to allow for a comparison between the two series of measurements. Paradoxically, the movement of the wake past the probe generates a pressure peak on the oscillogram. This may be explained by the fact that with fixed axes the dominant effect of this movement of the wake is a considerable increase in the angle α of the speed, while the modulus of the speed undergoes little change. As a result, the movement of the wake past the probe is accompanied by a considerable shift in the impact point, which, in the example given here, approaches the pressure inlet of the probe.

The results obtained with the pressure probe and with the hot-wire probe are compared in Fig. 14. A phase lead correction has been made in the measurements obtained with the pressure probe for this purpose to account for the lag between the time at which the pressure inlet detects a signal and the time at which the signal would be detected by a hot-wire probe occupying the position of the axis of the pressure probe.

The relative instants t/T, determined by both methods, /9
at which the fluctuations in the wake reach a maximum are in agreement.

Comparison of the two sets of values also shows that the width of the wake, indicated by the hot-wire probe, is on the same order of magnitude as the diameter of the pressure probe. As a result, this probe provokes an appreciable distortion of the wake, which may provide at least a partial explanation for the fact that the thickness of the wake derived from pressure measurements is greater and of lower amplitude than that resulting from the hot-wire probe.

Moreover, the provisional assumptions made in processing pressure data do not take the nonstationary nature of the flow into account.

For these reasons, the hot-wire measurements may be considered a closer approximation of reality.

Use of this device in an industrial compressor is problematic due to its fragility. On the other hand, the pressure probe is well-suited to use in an industrial assembly provided that its diameter is adequate (on the order of 8 mm) [8]. Research is being continued on the Cannes experimental assembly in order to improve the method of use of the pressure probe, especially by basing it on a comparison with hot-wire measurements.

4. Supersonic Measurements

4.1. Test Installation and Assemblies [9, 10, 11]

The measurements whose results will be presented shortly were performed on a supersonic compressor model (Fig. 15)

designed and built by the Energy Research Division of ONERA. Due to the use of freon[1] rather than air, supersonic flows can be obtained with this installation at a relatively low rotation speed and with extremely low drive power. The system operates on a closed circuit, the air flow being activated by the rotor tested. The latter is equipped with very slightly elongated blades (int. diam. 445 mm, ext. diam. 464 mm). This arrangement is especially well suited for visualization of the flow between blades by the Schlieren method, this being performed through a window machined into the inlet chamber.

In addition, a fixed hatch located on the inlet chamber upstream from the rotor is equipped with 12 piezoelectric ceramic pressure pickups. These are placed in cylindrical cavities machined into the hatch, but for safety reasons do not reach a level flush with the inside wall. The pressure is transmitted to the pickup through an opening in the shape of a truncated cone, filled with elastomer, so as to obtain a wide passband (Fig. 16).

4.2. Determining the Configuration of Shock Waves from the Rotor

The purpose of combining the use of Schlieren method visualization and pressure measurements on the inlet chamber upstream from the rotor was to relate the wall pressure map to the shock waves observed.

This was due to the fact that of these two methods, only the method of pressure measurement on the inlet chamber can

---

[1]The speed of sound in freon is approximately 130 m/s.

[2]The refraction index of freon is higher than that of air, which is an advantage in use of the Schlieren method.

actually be transposed to industrial turbines.

The results presented below were obtained with a rotation speed of 6500 rpm, an entrance Mach number, in relative axes, of M = 1.33, an upstream pressure of 57 mbar and a mean compression ratio of 1.4.

The signals from the various pickups are recorded in turn by means of the numerical mean finder. These recordings have a common origin which is defined by a rotor position reference.

Figure 17 shows the relative positions of the pickups and the rotor as measurement is begun, with two characteristic recordings from two pickups. The schematic representation of the shock waves from the rotor in this figure reveals the correspondence between the characteristics of the $\Delta p = f(t)$ diagram and the instants at which the pickup involved is affected by the shock waves.

With pickup A (diagram A), for example, an increase in pressure due to the recompression wave is followed by a pressure drop as the blade passes to the right of the pickup (Δp upper surface -- lower surface), a slight increase in pressure due to the shock wave generated by the following blade, etc.

With pickup B (diagram B), the shock waves can hardly be detected and the dominant element is still the movement of the blade itself, followed by a gradual increase in pressure in the inter-blade channel between the upper surface of one blade and the lower surface of the following blade.

Data recorded by the various detectors were used to set up a map of wall isobars, given in Fig. 18. The Schlieren photography of the flow illustrating this test, performed by the General Physics Division of ONERA, is given in Fig. 19. Superimposition of the tracing of the shock waves observed by the Schlieren method over the pressure map given in Fig. 18 shows that the shock waves appreciably coincide with areas where the proximity of the isobar curves reveals strong pressure gradients. It should be pointed out that a slight disagreement of the results may be partially attributed to distortion of the Schlieren photographs, since the flow was not strictly two-dimensional, and the fact that the two types of measurements involved different inter-blade channels.

5. Conclusions

The few experimental results given in this discussion have been chosen to illustrate the twofold orientation of the research conducted:

-- comparison of measurements with theoretical results;
-- development of methods of measurement which may be transposed to industrial aeronautic turbines.

These examples are not restrictive, and other measuring /11 procedures are being researched and developed. Specifically these include nonstationary measurement of local friction by means of "hot-film" wall pickups, anemoclinometric measurement by means of "hot-film" probes, which are more durable than hot-wire probes and can be used in an industrial environment, miniaturization of pressure probes, etc.

Some of the methods presented cannot be used industrially, but their use in laboratory setups makes it possible to develop and check the performances of simpler devices which could be used for measurements on real turbines or to control methods of computation.

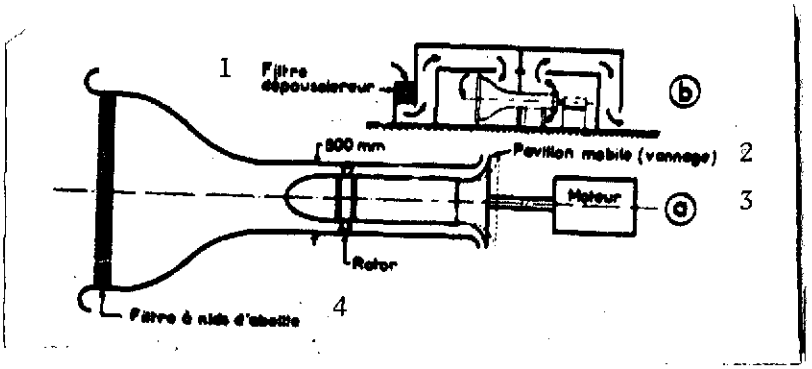

Fig. 1. a) Schematic view of the Cannes test assembly.
b) Cross-sectional view of sound-proofed site: air intake and discharge circuits.

Key: 1. Dedusting filter
2. Movable bellmouth (vanning)
3. Motor
4. Honeycomb filter

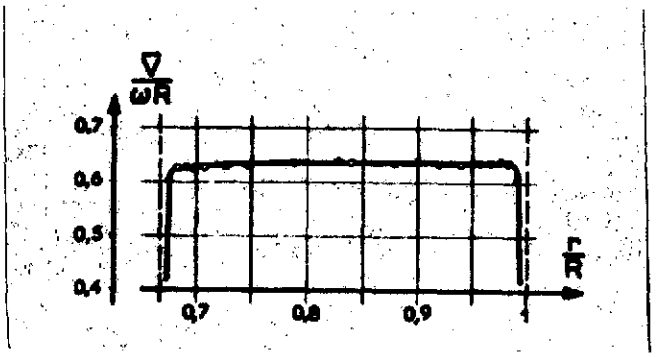

Fig. 2. Radial distribution of average speed $\overline{V}$ at a distance of 12 mm upstream from rotor (prerotation of the airflow is negligible).
N = 3000 rpm

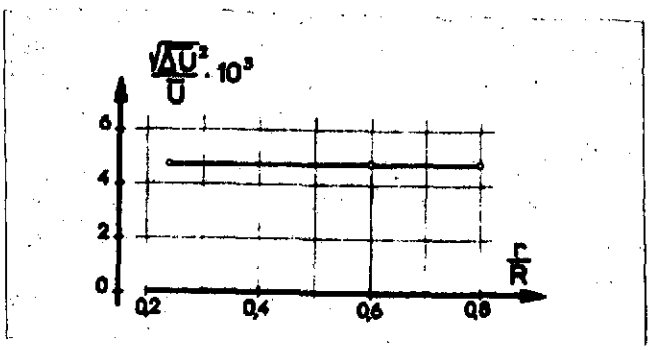

Fig. 3. Turbulence ratio in the outlet cross-section of the air manifold, determined by means of a hot-wire probe.
N = 3000 rpm.

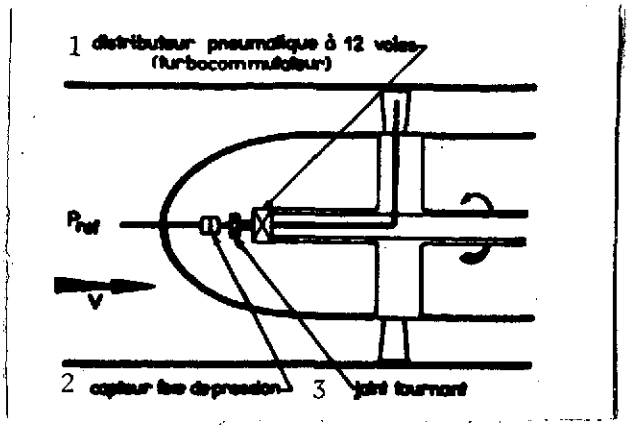

Fig. 4. Diagram of test assembly used for stationary pressure measurements on rotor blades.

Key: 1. 12-channel pneumatic distributor (turbo commutator)
2. Pressure pickup
3. Rotating joint

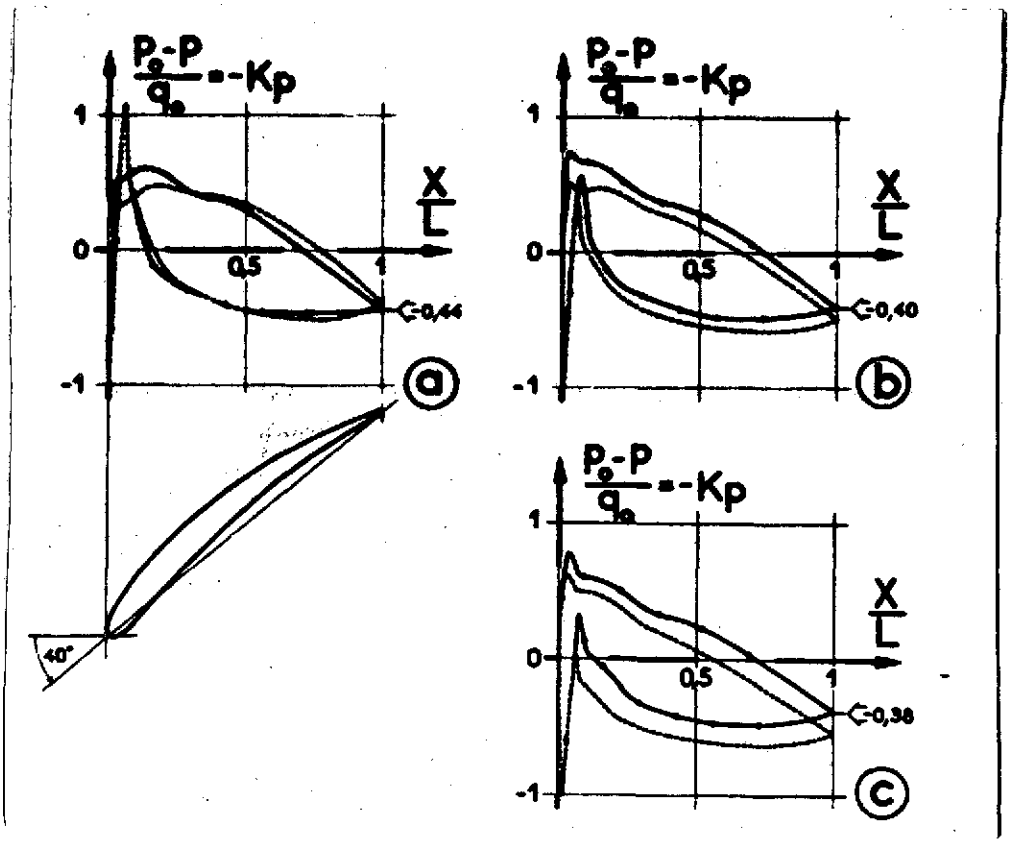

Fig. 5. Pressure distribution on a rotor blade; N = 3000 rpm.
a) r/R = 0.708 experimental curve
b) r/R = 0.834 --------- computation (ideal fluid)
c) r/R = 0.918 value of $(p_o - p)/Q_o$ determined by radial measurement downstream from the rotor.

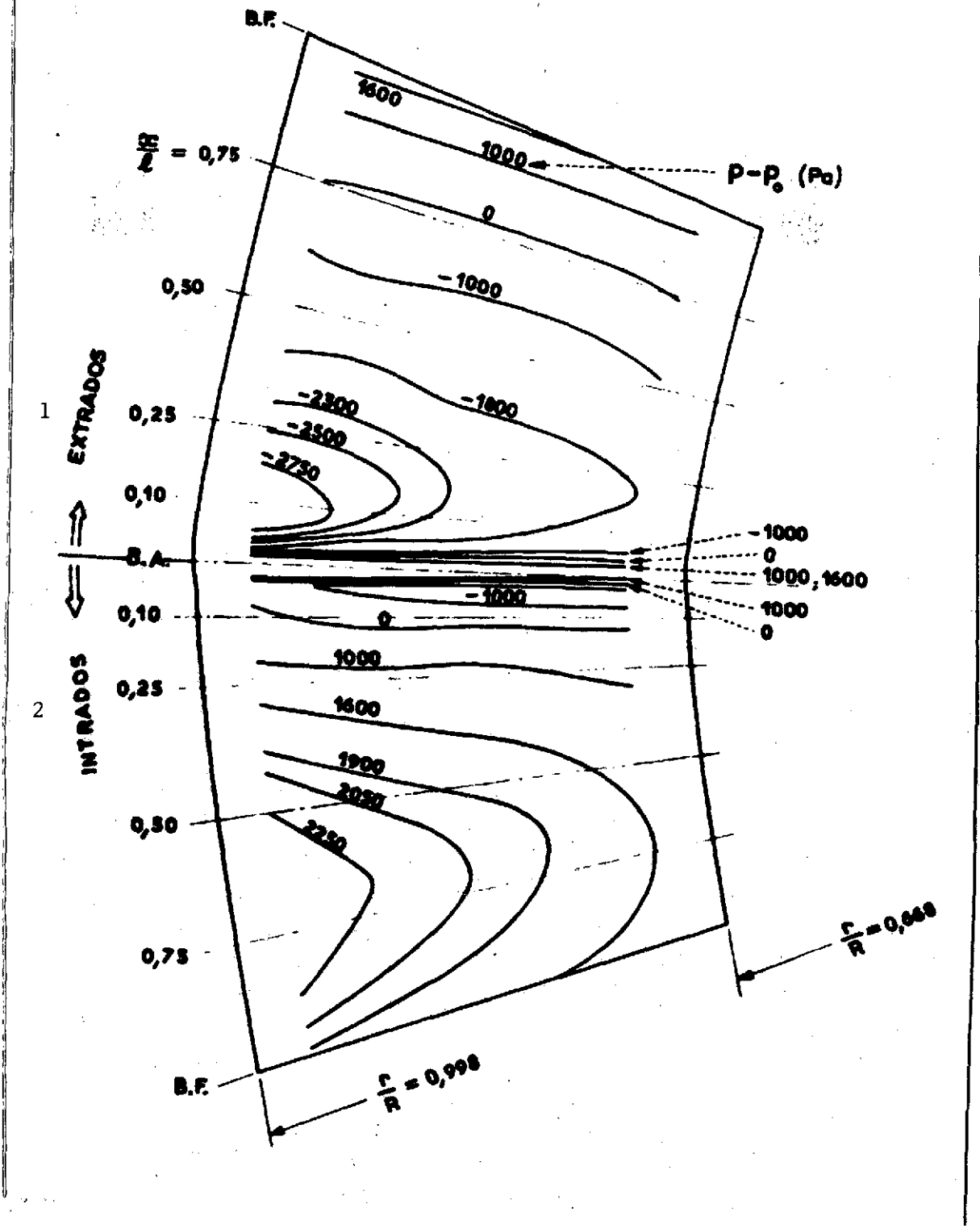

Fig. 6. Map of isobars on the developed surface of the rotor blade. N = 3000 rpm.

Key: 1. Blade upper surface
2. Blade lower surface

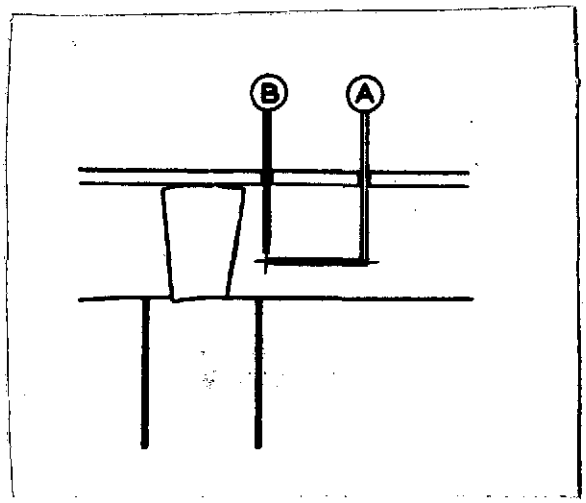

Fig. 7. Diagram of arrangement of hot-wire probes.
A measurement of V
B determination of α

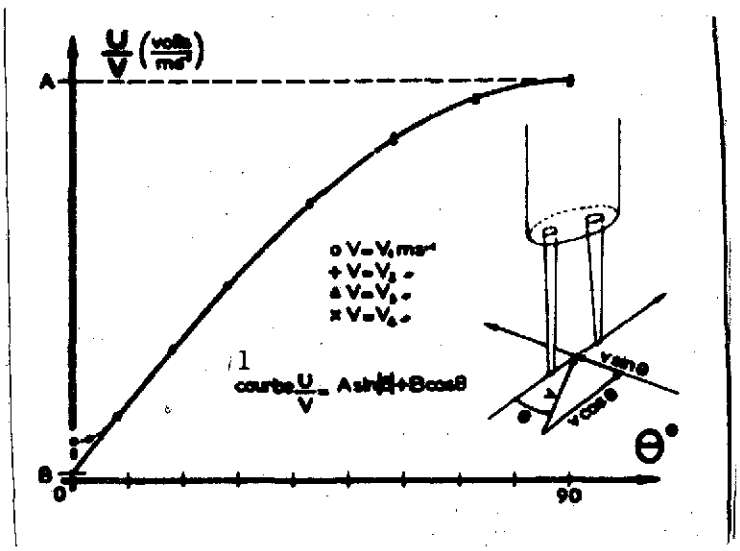

Fig. 8. Directional calibration of hot-wire probe in wind tunnel.

Key: 1. Curve

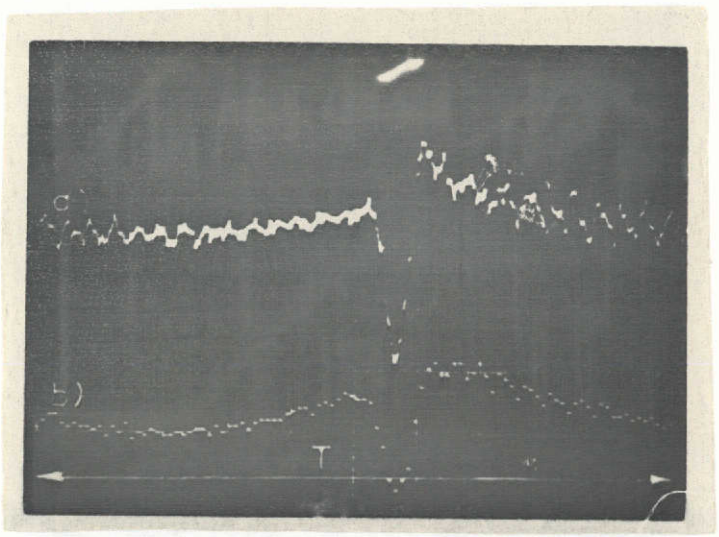

Fig. 9. Response of hot-wire probe to a speed fluctuation of 6.5 m/s due to the wake.
a) Direct response (one pass of blade);
b) Mean curve (900 passes of a single blade).

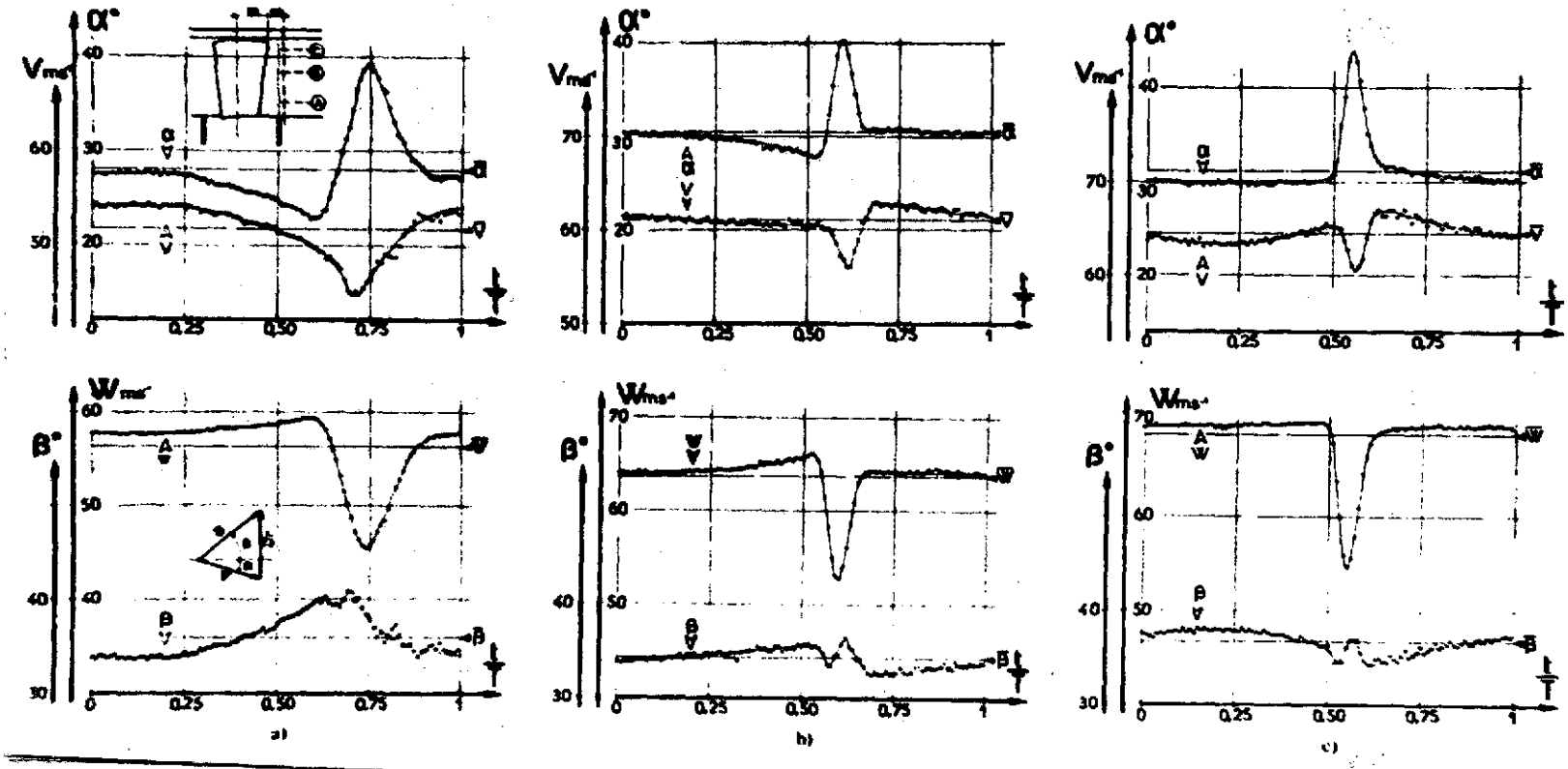

Fig. 10. Hot-wire anemoclinometric measurements downstream from rotor. Speed and direction of flow:
a) At point A: r/R = 0.728
b) At point B: r/R = 0.852
c) At point C: r/R = 0.948

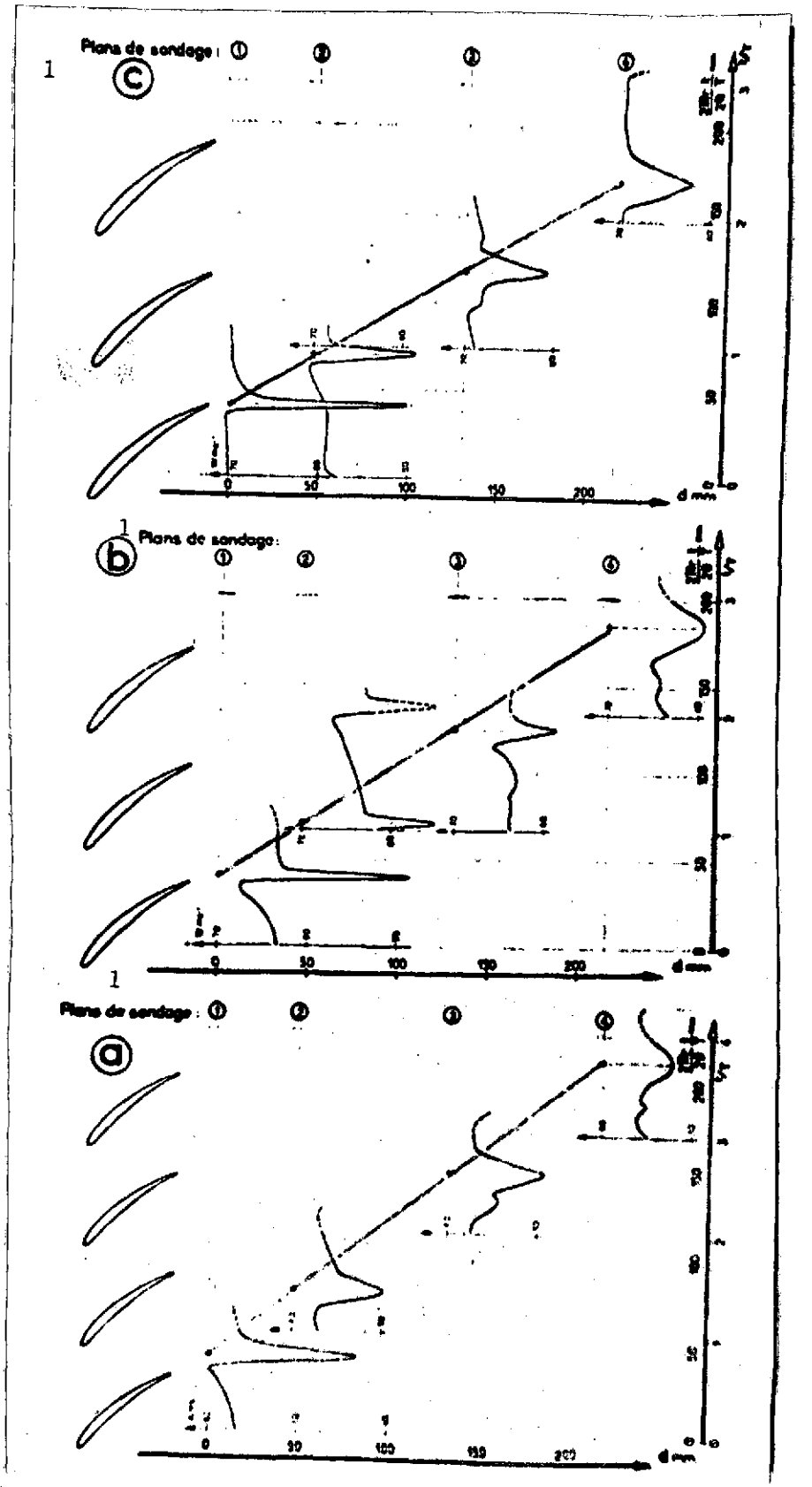

Fig. 11. Path and diffusion of the wake of a rotor blade represented at a constant relative radius.
a) r/R = 0.728
b) r/R = 0.852
c) r/R = 0.948

Key: 1. Planes of measurement

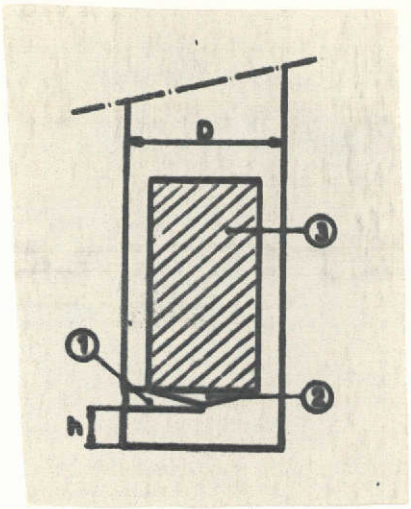

Fig. 12. Diagram of cylindrical pressure probe (diam. = 8 mm; h = 2 mm).
(1) Pressure inlet opening; diam. = 1 mm
(2) Dead space. Volume ≈ 1 m^3
(3) Pressure pickup; diam. = 6 mm

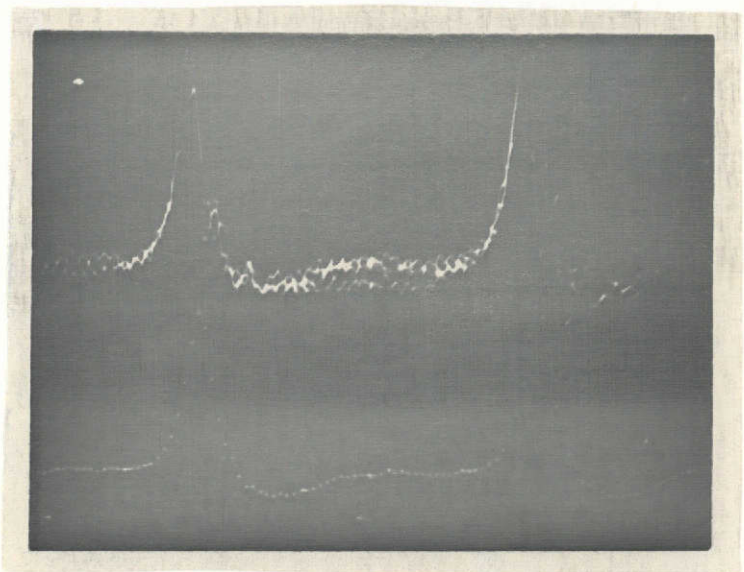

Fig. 13. Response of pressure probe (θ_1 = = $+30^o$) to a pressure fluctuation of 15 mbar. T = 1 ms.
a) Direct response (three passes of the same two successive blades)
b) Mean curve (900 passes of the same two blades)

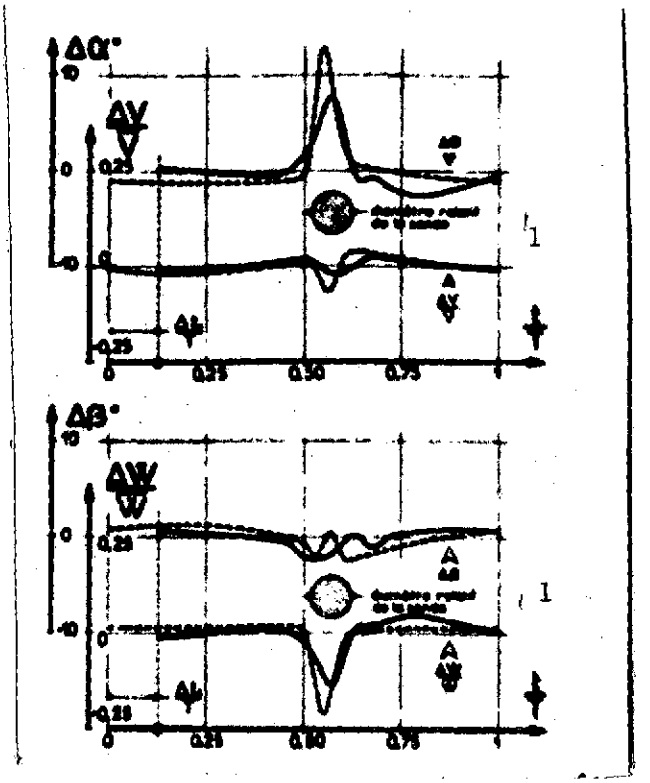

Fig. 14. Comparison of results of measurement. r/R = 0.948.
----- hot-wire probe
——— pressure probe

Key: 1. [Word illegible] diameter of probe

/20

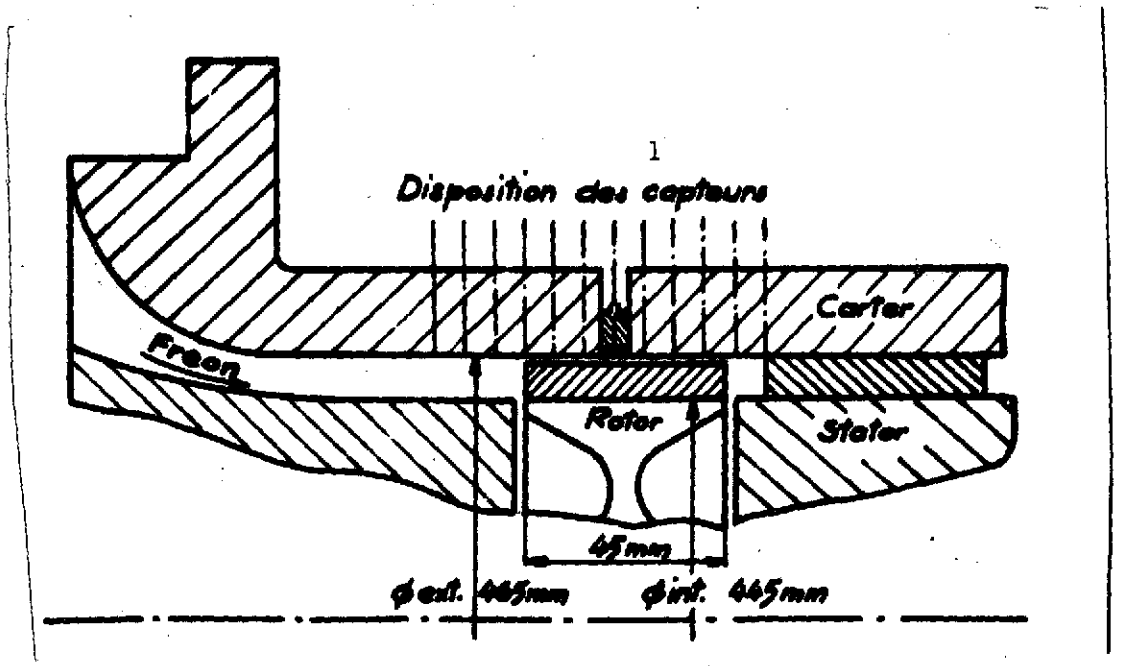

Fig. 15. Longitudinal cross section of the supersonic compressor model designed by the Energy Research Division of ONERA.

Key: 1. Arrangement of pickups; 2. inlet chamber.

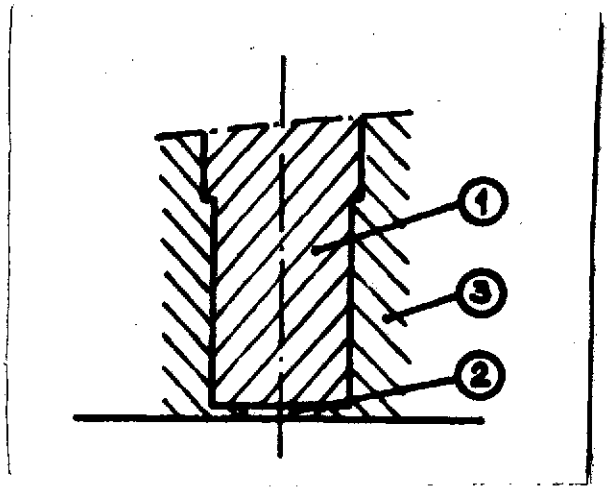

Fig. 16. Wall assembly of pressure pickup.
(1) Pressure pickup
(2) Elastomer
(3) Inlet chamber of model

/21

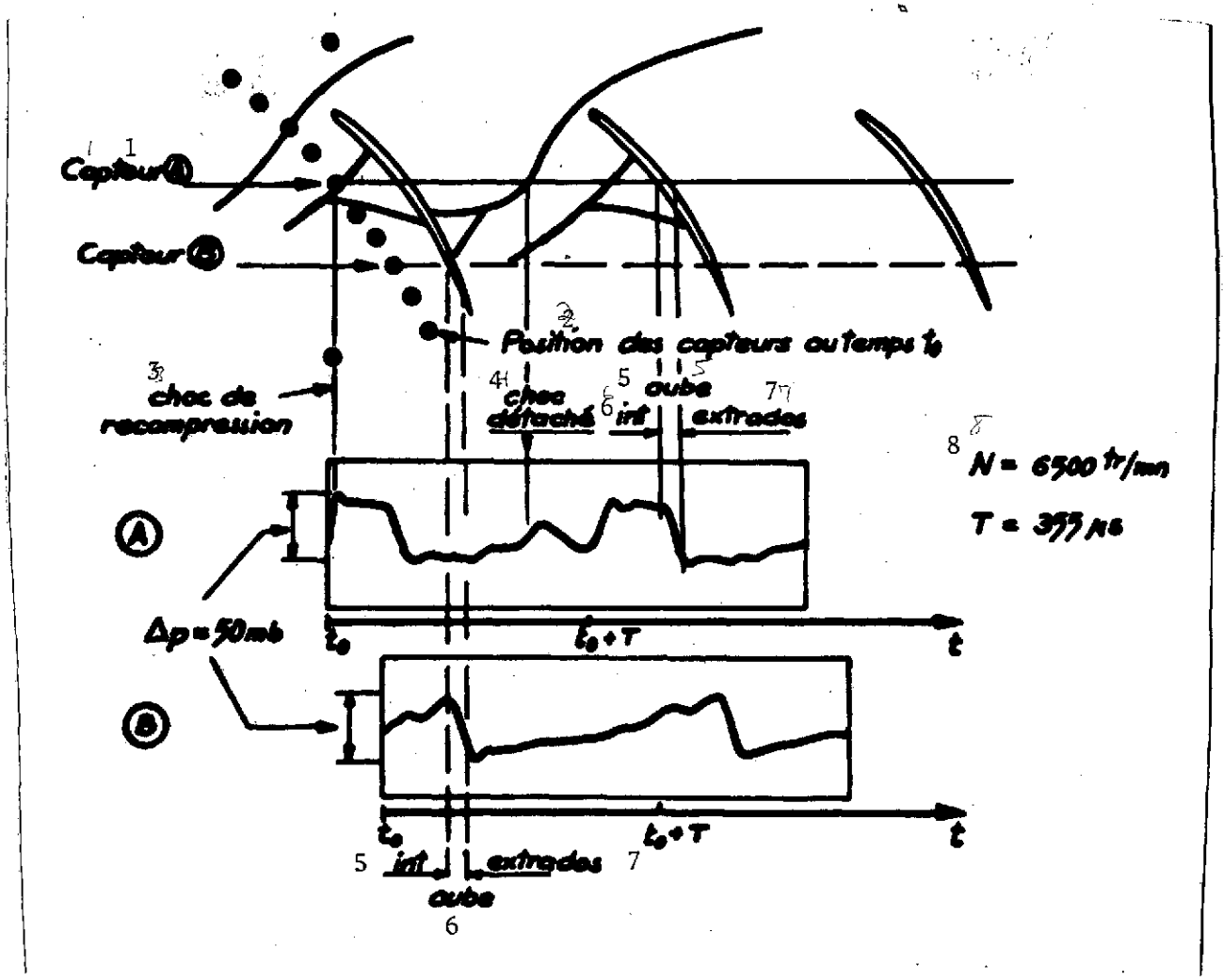

Fig. 17. Arrangement of pickups and relative position of rotor at beginning of measurement. Examples of recordings.

[Key on following page.]

(Key to Fig. 17):

1. Pickup A (typ.)
2. Position of pickups at time t_o
3. Recompression impact
4. Detached impact
5. Blade
6. Lower surface
7. Upper surface
8. N = 6500 rpm

Fig. 18 [on following page]:

Map of wall isobars (mbar). Comparison with shock waves observed by the Schlieren method (shaded area).

Key: 1. Upstream flow

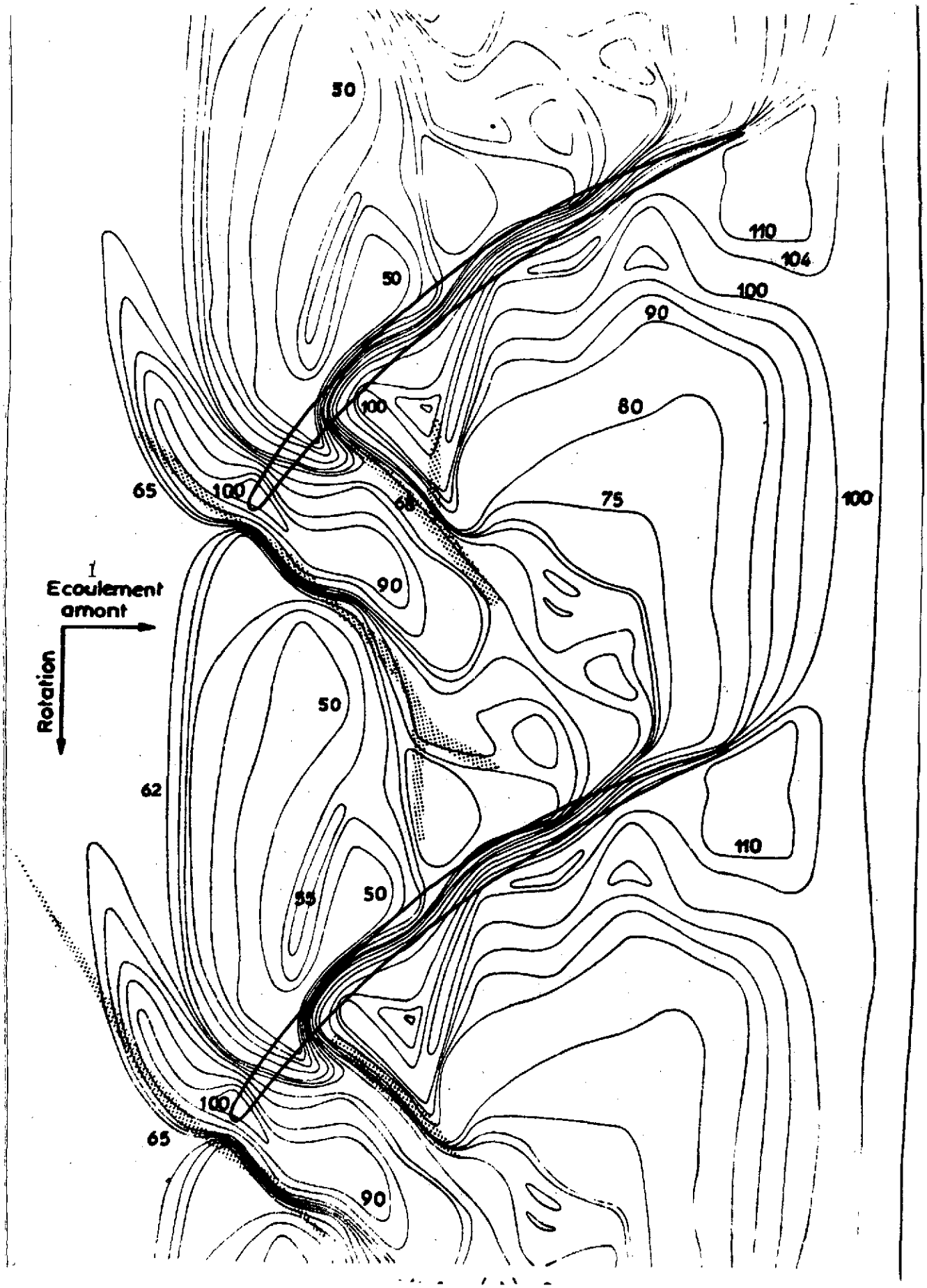
50
110
104
50
100
90
100
80
65
100
75
100
1
Ecoulement
amont
90
Rotation
50
62
110
55
50
100
65
90

Fig. 19. Schlieren photograph of airfflow in rotor. N = 6500 rpm. M = 1.33. p_o = = 57 mbar.

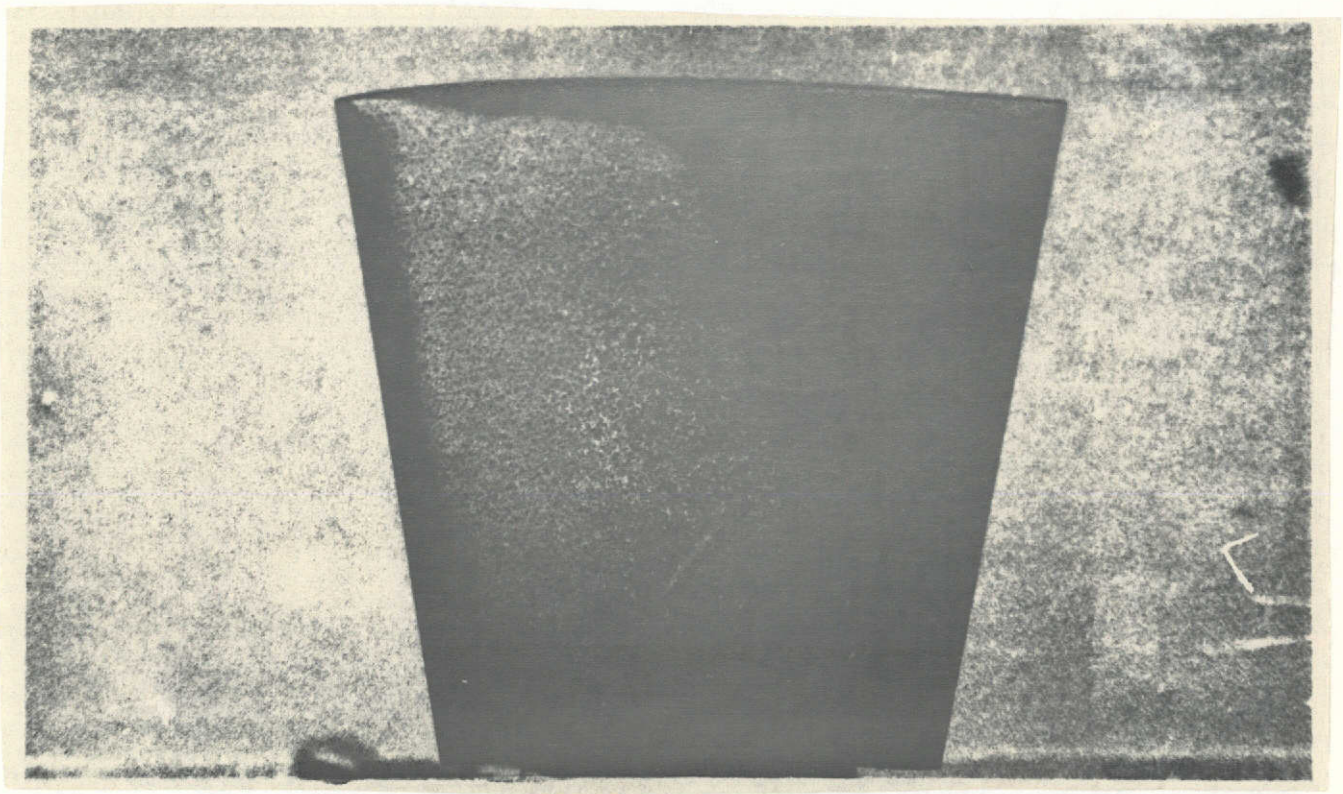

Fig. 20. Visualization of boundary layer transition on blade upper surface by the sublimating coating method.

REFERENCES

1. de Sievers, A. and R. Larguier, "Device for measurement of the aerodynamic flow inside an axial turbine," ATMA Session, Paris, 1973.

2. Le Bot, Y., "The role of the turbulent boundary layer in axial compressors," Euromech 33, Berlin (25-27 Sept. 1972).

3. Rollin, G. and F. Suif, "Improvements in methods for pressure measurement at several points on a rotating component of a turbine," French Patent Request No. 71-25 707, 13 July 1971.

4. Meauzé, G. and J.J. Thibert, "Method of experimental analysis of highly deflected supersonic blade grids," ATMA Session, Paris, 1972.

5. Larguier, R., G. Fasso, and M. Scherer, "Study of periodic pressure fluctuations on the fixed blades of a high-power axial compressor," ATMA Session, Paris, 1971.

6. Lambourion, J. and R. Larguier, "Description, calibration and example of use of a pressure pickup with short response time," La Recherche Aérospatiale, No. 133 (Nov./Dec. 1969).

7. Lopez, J. and Ch. d'Humières, "Dynamic calibration of pressure pickups by periodic plateaus," La Recherche Aérospatiale, No. 1972-3 (May/Jun.).

8. Larguier, R. and C. Ruyer, "Method for experimental analysis of the nonstationary flow inside a supersonic aeronautic compressor," La Recherche Aérospatiale, No. 1972-6 (Nov./Dec.).

9. Fabri, J. and J. Reboux, "Similarity of performances of compressors using different thermodynamic gases," ATMA Session, Paris, 1971.

10. Philbert, M. and G. Fertin, "Visualization devices for fixed or rotating annular grid wind tunnels," La Recherche Aérospatiale, No. 1971-2 (Mar./Apr.).

11. Fabri, J., "Visualization of flow in a supersonic axial compressor," L'Aéronautique et l'Astronautique, No. 17 (1/1970).